

# Calculated Unconventional Superconductivity via Charge Fluctuations in Kagome Metal $\text{CsV}_3\text{Sb}_5$

Yuan Tian, Sergey Y. Savrasov

*Department of Physics, University of California, Davis, CA 95616, USA*

Electrons on Kagome lattice exhibit a wealth of features including Dirac points, van Hove singularities and flatbands. When the Fermi level is placed at the van Hove saddle point, the Fermi surface is perfectly nested and a rich variety of electronic instabilities is known to occur. The material realization of such scenario is a recently discovered Kagome system  $\text{CsV}_3\text{Sb}_5$  whose superconductivity near charge–density wave instability at low temperatures points to an unconventional, non–electron–phonon, pairing mechanism. Here we use a recently developed combination of density functional theory with momentum and frequency–resolved self–energies deduced from the so–called fluctuational–exchange–type random phase approximation to study charge fluctuation mediated pairing tendencies in  $\text{CsV}_3\text{Sb}_5$ . Based on our numerical diagonalization of the BCS gap equation, two competing solutions emerge from these calculations with  $A_{1g}$  (anisotropic s–wave–like) and  $B_{2g}$  ( $d_{x^2-y^2}, d_{xy}$ –like) symmetries of the superconducting order parameter. Our evaluated Eliashberg spectral functions  $\alpha^2F(\omega)$  are purely due to electronic correlations; they were found to be strongly peaked in the vicinity of frequency 7 meV that sets the scale of charge fluctuations. The superconducting coupling constants for the leading pairing channels are estimated as a function the nearest neighbor Coulomb interaction  $V$ , a well–known prime parameter of the extended Hubbard model. They were found in the range of 0.2–0.4 depending on  $V$ . We evaluate the superconducting  $T_c$  close to the values that are observed experimentally that point to the charge fluctuations to provide a substantial contribution to the pairing mechanism in  $\text{CsV}_3\text{Sb}_5$ .

PACS numbers:

Unconventional mechanisms of superconductivity have always been a subject of intense interest in the research of quantum materials with such much celebrated examples as high–temperature superconducting cuprates[1], ironates[2] and recently, nickelates[3], where antiferromagnetic spin fluctuations are thought to be the primary source of the Cooper pairing[4, 5]. There is however another class of systems, for which the proximity not to the spin but to the charge density wave (CDW) instability can be linked to the formation of the Cooper pairs. The most notable example is the 30K superconductivity in potassium doped  $\text{BaBiO}_3$ [6] where the Bi ions in the parent insulating compound exist in a charge disproportionated state.

The discovery[7] of a family of non–magnetic metals  $\text{CsV}_3\text{Sb}_5$ ,  $\text{KV}_3\text{Sb}_5$ ,  $\text{RbV}_3\text{Sb}_5$  with vanadium ions forming a Kagome lattice framework is currently generating a great interest due to the appearance of multiple charge–ordered states at high temperatures[8], as well as of bulk superconductivity with  $T_c=2.5\text{K}$  in  $\text{CsV}_3\text{Sb}_5$ [9] and with  $T_c=0.8\text{K}$  in  $\text{KV}_3\text{Sb}_5$ [10] whose normal state electronic structure categorizes these systems as  $Z_2$  topological metals[9]. Remarkably, pressure dependent studies of  $\text{CsV}_3\text{Sb}_5$  have shown that the CDW order can be suppressed by applying a 2GPa pressure which leads to the enhanced  $T_c$  value of 8K[11].

Although the observed small values of  $T_c$  are well within the reach of the conventional mechanism, theoretically calculated electron–phonon coupling constants are generally found to be small[12]. There exists a factor–of–two discrepancy between predictions of the theory and the kinks in the band dispersions of the Fermi

electrons measured by Angle Resolved Photoemission Spectroscopy (ARPES)[13]. More importantly, several experiments performed on  $\text{CsV}_3\text{Sb}_5$  point to a strong momentum dependence of the superconducting energy gap. Scanning tunneling microscopy (STM)[14–16] has detected a V–shaped density of superconducting states, indicating the presence of nodes in the order parameter. On the other hand, the magnetic penetration depth experiments[17–20] suggest nodeless but anisotropic superconductivity. Despite been presently controversial, both observations are incompatible with the constant energy gaps which are observed in the vast majority of electron–phonon superconductors and indicate the unconventional nature of the pairing state.

Electronic instabilities on the Kagome lattice have been a subject of recent theoretical works. Its minimal three–band model of itinerant electrons with short–range hoppings is known for a wealth of features including the existence of a Dirac point at the Brillouin Zone (BZ) point  $K=(1/3, 1/\sqrt{3}, 0)2\pi/a$  of hexagonal lattice, a van Hove singularity (VHS) at the point  $M=(0, 1/\sqrt{3}, 0)2\pi/a$ , and a dispersionless (flat) band for all wavevectors. When the Fermi level is pinned at the VHS, the Fermi surface is represented by a perfect hexagon and becomes nested along the whole line  $\Gamma M$  of the BZ. In this regime, the extended Hubbard model with the on–site and intersite Coulomb interactions  $U$  and  $V$  has been studied using a variational cluster approach[21] and a functional renormalization group theory[22, 23]; it reveals a rich variety of quantum phases including the appearance of magnetic order, charge density waves and superconductivity. The symmetries of the superconducting order pa-

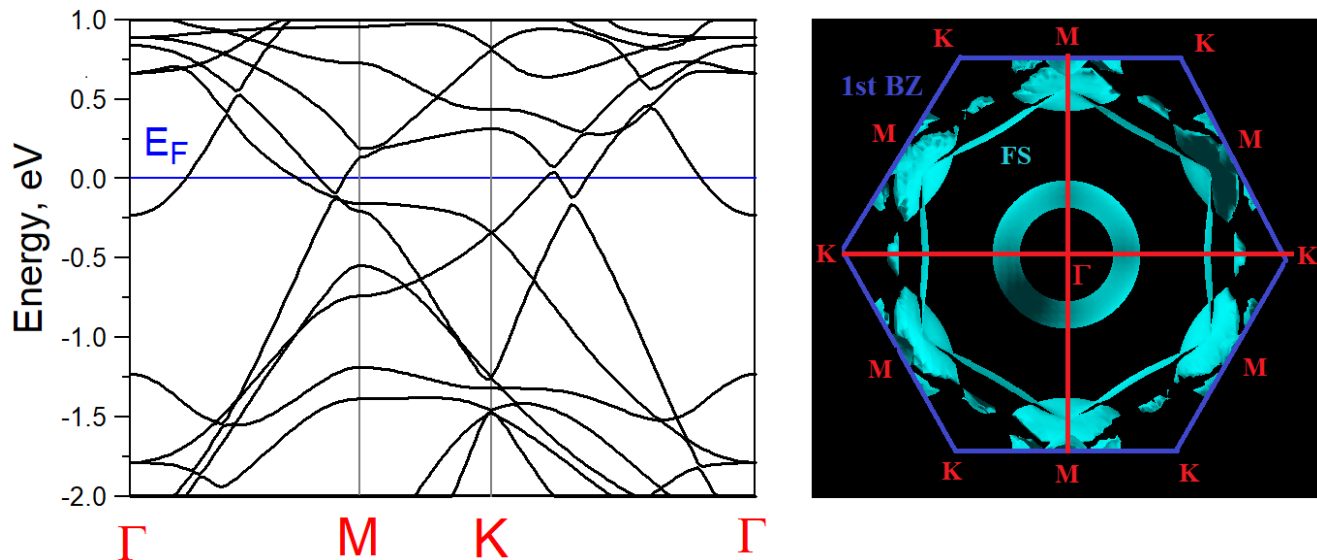


FIG. 1: Density functional calculations for  $\text{CsV}_3\text{Sb}_5$ : (a) the electronic energy bands with clearly distinguished VHS saddle point below the Fermi level at  $M$ , the Dirac point at  $K$ , and nearly dispersionless bands at 1 eV above the  $E_F$ . b) The Fermi surface with the visible hexagonal pattern characteristic of the tight-binding model on Kagome lattice known for its nesting features along  $\Gamma M$ .

parameter recovered from these studies include anisotropic  $s$ -wave state and  $d_{x^2-y^2}, d_{xy}$  two-fold degenerate state, for which a fully gapped chiral combination  $d_{x^2-y^2} + id_{xy}$  was found to be energetically most favorable. Later studies of the Kagome based tight-binding models included renormalization group supplemented with Landau theory analysis of various charge density wave modulations seen in  $\text{CsV}_3\text{Sb}_5$  [24], and the low-energy effective model for various CDW induced flux phases [25] to explain the observed time-reversal symmetry breaking in  $\text{KV}_3\text{Sb}_5$  [26].

To address the issue of unconventional pairing state in  $\text{CsV}_3\text{Sb}_5$ , here we use our recently developed approach [27, 28] that evaluates superconducting pairing functions directly from first-principle electronic structure calculations of the studied material using realistic energy bands and wave functions available from density functional theory (DFT) [29]. The electronic self-energies are calculated for a manifold of correlated electrons similar to as it is done in popular DFT+DMFT approach [30], but they acquire full momentum and frequency resolution within this method, which diagrammatically corresponds to the so-called fluctuational-exchange (FLEX) type [31] random phase approximation (RPA) incorporating all type of nesting-driven instabilities in the charge and spin susceptibilities. The description of unconventional superconductors in a realistic material framework without reliance on the tight-binding approximations of the electronic structures became possible using this DFT+FLEX(RPA) method. Our most recent applications [28] to  $\text{HgBa}_2\text{CuO}_4$ , a prototype single-layer cuprate superconductor, easily recovered a much celebrated  $d_{x^2-y^2}$  symmetry of the order parameter, and the prediction of competing  $s_{\pm}, d_{xy}$  pairing states was given [32] for a recently discovered high-temperature su-

perconducting nickelate compound  $\text{La}_3\text{Ni}_2\text{O}_7$ .

The main physical picture emergent from the experimental data for  $\text{CsV}_3\text{Sb}_5$ , is that a nearly singular behavior in the charge susceptibility plays an important role in the 2.5K superconductivity at ambient pressure [9], where a variety of charge ordered phases is seen at higher temperatures [16], and that the rise of  $T_c$  to 8K by applying a pressure of 2GPa [11] is related to the suppression of the CDW. This prompts us to consider the on-site and the neighboring-site Coulomb interaction parameters  $U$  and  $V$  for vanadium  $d$ -electrons to be of the same order of magnitude with the parameter  $V$  tuning the system to the instability point to allow strong charge fluctuations.

To uncover whether such charge fluctuational mechanism can explain or contribute to superconductivity in  $\text{CsV}_3\text{Sb}_5$ , we numerically evaluate the pairing interaction describing the scattering of the Cooper pairs as a function of the intersite  $V$  while fixing the on-site  $U$  to its representative value of 0.1 Ry (=1.36 eV). This pairing function is then used to exactly diagonalize the linearized Bardeen-Cooper-Schrieffer (BCS) gap equation on a three-dimensional  $k$ -grid of the Fermi points in the BZ. The highest eigenvalue  $\lambda_{\text{max}}$  deduced from this procedure represents a coupling constant similar to the electron-phonon  $\lambda$  in conventional theory of superconductivity. We generally find  $\lambda_{\text{max}}$  to be negligible unless  $V$  is tuned to the close proximity to the CDW occurring in our procedure at around 1.8 eV. We recover two nearly degenerate solutions of the superconducting order parameter from these calculations: first, of  $B_{2g}$  ( $d_{x^2-y^2}, d_{xy}$ -like) and, second, of  $A_{1g}$  (anisotropic  $s$ -wave-like) symmetry. Using spectral representation for the pairing interaction, we evaluate charge fluctuation induced Eliashberg spectral functions  $\alpha^2F(\omega)$  which were found to be

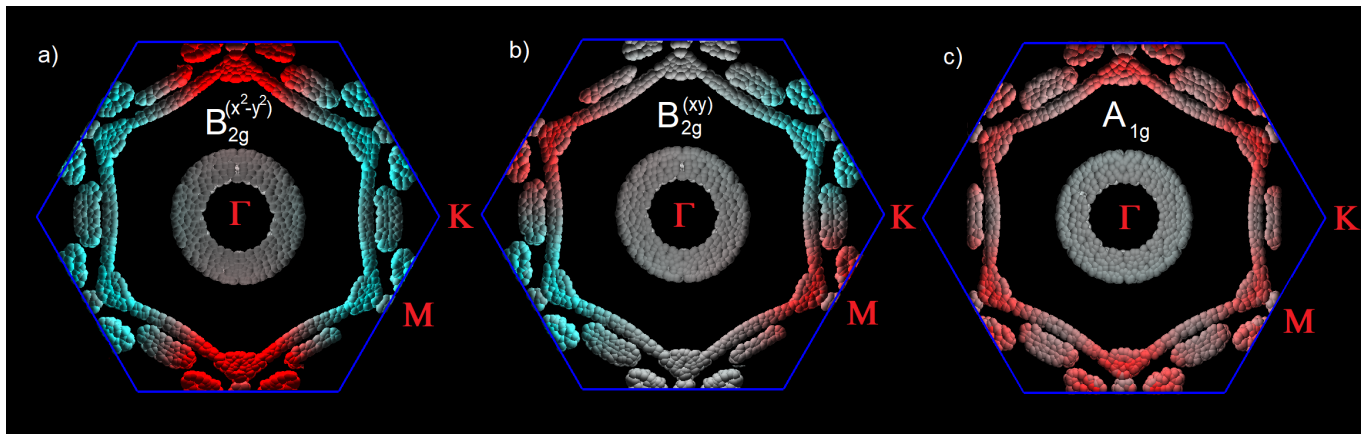


FIG. 2: Calculated superconducting energy gap  $\Delta(\mathbf{k}j)$  for singlet pairing in  $\text{CsV}_3\text{Sb}_5$  using numerical solution of the linearized BCS gap equation with the pairing interaction evaluated using the DFT+FLEX(RPA) approach. Blue/red color corresponds to the negative/positive values of  $\Delta(\mathbf{k}j)$ . Plots a) and b) correspond to  $B_{2g}$  symmetry ( $d_{x^2-y^2}$  and  $d_{xy}$  like); plot c) corresponds to  $A_{1g}$  symmetry (anisotropic s-wave-like).

strongly peaked at the frequency 7 meV. To allow estimates for the  $T_c$ , charge fluctuational contribution to the electronic mass enhancement  $m^*/m_{\text{band}} = 1 + \lambda_{cf}$  is evaluated to produce the effective coupling constants  $\lambda_{eff} = \lambda_{\text{max}}/(1 + \lambda_{cf})$  for the leading pairing channels. These were found in the range of 0.2–0.4 depending on  $V$  and leads to the  $T_c$  estimates close to the values that are observed experimentally.

We perform our density-functional electronic-structure calculations using the full potential linear muffin-tin orbital method[33]. The result for the electronic energy bands is shown in Fig. 1(a) along major high-symmetry directions of the hexagonal BZ. In accord with the previous study [9], it shows the band dispersions in the vicinity of the Fermi level  $E_F$  originating from the vanadium d-orbitals. Despite their complexity, the VHS saddle point just below the Fermi level at point M, the Dirac point at K, and the nearly dispersionless bands at 1 eV above the  $E_F$  are clearly distinguished. The Fermi surface shown in Fig. 1(b) is quasi-two dimensional with the visible hexagonal pattern. All these features are characteristic of the minimal tight-binding model on Kagome lattice known for its nesting along  $\Gamma M$ .

We further utilize our DFT+ FLEX(RPA) method to evaluate the charge fluctuation mediated pairing interaction. The Fermi surface is triangularized onto small areas described by about 6,000 Fermi surface momenta for which the matrix elements of scattering between the Cooper pairs are calculated using the approach described in Ref. [28]. The linearized BCS gap equation is then exactly diagonalized and the set of eigenstates is obtained for both singlet ( $S = 0$ ) and triplet ( $S = 1$ ) Cooper pairs. The highest eigenvalue  $\lambda_{\text{max}}$  represents the physical solution and the eigenvector corresponds to superconducting energy gap  $\Delta(\mathbf{k}j)$  where  $\mathbf{k}$  is the Fermi surface momentum and  $j$  numerates the Fermi surface sheets.

We find that there are three highest eigenvalues that

appear very close to each other. The leading pairing channel is two-fold degenerate and the subleading one is non-degenerate with its eigenvalue appearing only within 6% of the maximum eigenvalue. We analyze the behavior of  $\Delta(\mathbf{k}j)$  as a function of the Fermi momentum using the values of  $U=1.36$  eV and  $V = 1.75$  eV. The solutions are related to the spin singlet states, and Fig. 2(a),(b) shows the behavior of the two-fold degenerate  $\Delta(\mathbf{k}j)$ , while Fig. 2(c) corresponds to the non-degenerate one. One can see that the two-fold degenerate eigenstate shows the behavior corresponding to the  $B_{2g}$  symmetry ( $d_{x^2-y^2}$ -like in a) and  $d_{xy}$ -like in b), The plot distinguishes negative and positive values of  $\Delta(\mathbf{k}j)$  by blue and red colors while zeros of the gap function are colored in grey. The non-degenerate solution of  $A_{1g}$  symmetry is plotted in Fig. 2(c) where the gap function is strongly anisotropic exhibiting its maxima close to the M points of the BZ and nearly zeroes in between.

We can gain additional insight on the behavior of the eigenvalues by varying the intersite Coulomb interaction  $V$ . We first evaluate the divergency of the charge susceptibility that occurs at  $V_{CDW}$  slightly less than 1.77 eV. We use the range of values  $V < V_{CDW}$  to extract from the BCS gap equation the behavior of the highest eigenstates  $\lambda_{\text{max}}$  and their symmetries as a function of  $V$ . We find that both  $B_{2g}$  and  $A_{1g}$  symmetries robustly dominate over all other solutions with the two-fold degenerate  $B_{2g}$  state to be only 6% larger than the non-degenerate one. Obviously, however, if the electron-phonon coupling constant  $\lambda_{e-p} \approx 0.25$ [12] is taken into account, the  $A_{1g}$  pairing will become the leading one.

It is interesting to discuss the dependence of  $\lambda_{\text{max}}$  as a function of  $V$  that is shown in Fig. 3 (squares connected by black lines). We see that the values of  $\lambda_{\text{max}}$  are very small unless  $V$  approaches closely to  $V_{CDW}$  where it reaches the values 0.2–0.6. This indicates that the charge fluctuations produce essential contribution to the pairing only in the immediate vicinity of the CDW instability.

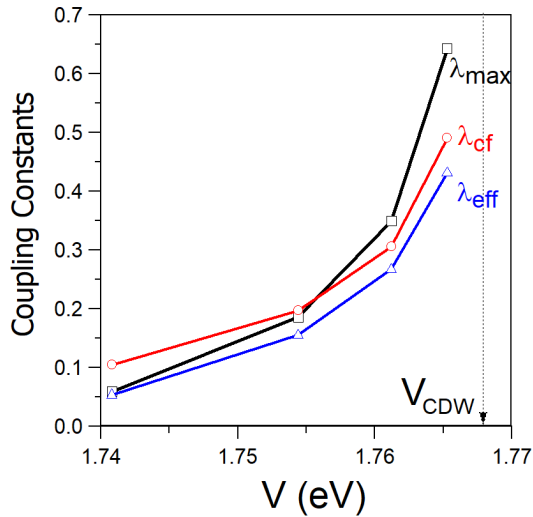


FIG. 3: Calculated using DFT+FLEX(RPA) method dependence of the highest eigenvalue  $\lambda_{\max}$  (squares connected by black lines) corresponding to  $B_{2g}$  symmetry of the linearized BCS equation, as well as charge fluctuational mass enhancement parameter  $\lambda_{cf}$  (circles connected by red lines) as a function of the inter-site Hubbard interaction  $V$  close to its critical value  $V_{CDW} = 1.768\text{eV}$  for the vanadium d-electrons in  $\text{CsV}_3\text{Sb}_5$ . The effective coupling constant  $\lambda_{eff} = \lambda_{\max}/(1 + \lambda_{cf})$  determining the strength of the charge fluctuational pairing is also shown (triangles connected by blue lines).

To get insight on possible range of critical temperatures that can be obtained using the charge fluctuation mechanism, we recall that it is not the eigenvalue  $\lambda_{\max}$  but the effective coupling constant  $\lambda_{eff}$  enters the BCS  $T_c$  expression:  $T_c \approx \omega_{cut} \exp(-1/\lambda_{eff})$ . If we neglect phonons, the cutoff frequency  $\omega_{cut}$  is thought here due to charge fluctuations, and  $\lambda_{eff}$  incorporates the effects associated with the mass renormalization describing by the parameter  $\lambda_{cf}$ . It should also be weakened somewhat by the Coulomb pseudopotential  $\mu_m^*$  which should refer to the same pairing symmetry  $m$  as  $\lambda_{\max}$ :

$$\lambda_{eff} = \frac{\lambda_{\max} - \mu_m^*}{1 + \lambda_{cf}} \quad (1)$$

The mass enhancement can be evaluated as the Fermi surface (FS) average of the electronic self-energy derivative taken at the Fermi level

$$\lambda_{cf} = -\left\langle \frac{\partial \Sigma(\mathbf{k}, \omega)}{\partial \omega} \Big|_{\omega=0} \right\rangle_{FS} \quad (2)$$

Our calculated dependence of  $\lambda_{cf}$  on  $V$  is shown in Fig. 3 (circles connected by red lines). It is seen to exhibit the behavior very similar to  $\lambda_{\max}$ : the values of  $\lambda_{cf}$  are found to be modest unless  $V$  lies in the vicinity of  $V_{CDW}$  where  $\lambda_{cf}$  is found between 0.2 and 0.5.

To give estimates for the effective coupling constant,  $\lambda_{eff}$ , we notice that  $\mu_m^*$  is expected to be very small for the pairing symmetries different from the standard s-wave [34]. We therefore expect this parameter to be zero

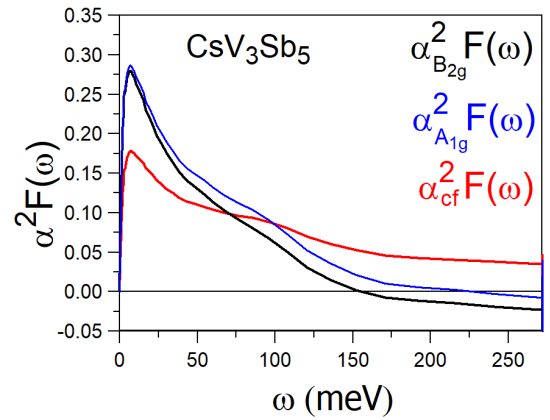


FIG. 4: Calculated Eliashberg spectral functions  $\alpha^2 F(\omega)$  due to charge fluctuations for the leading pairing symmetries,  $B_{2g}$  (black lines), and  $A_{1g}$  (blue lines) of the superconducting order parameter in  $\text{CsV}_3\text{Sb}_5$ . The spectral function  $\alpha_{cf}^2 F(\omega)$  whose inverse frequency moment produces charge fluctuational mass enhancement parameter  $\lambda_{cf}$  is shown in red.

for the  $B_{2g}$  pairing state. The plot of  $\lambda_{eff} = \lambda_{\max}/(1 + \lambda_{cf})$  vs.  $V$  is shown in Fig. 3. One can see that the range of these values is between 0.2 and 0.4 in the proximity to the CDW.

One can easily incorporate the electron-phonon  $\lambda_{e-p} \approx 0.25$ [12] into this discussion. The kink in the band dispersion of the Fermi electrons will become a sum  $\lambda_{cf} + \lambda_{e-p}$ . It essentially doubles as compared to the individual contributions due to phonons or charge fluctuations and will match the recent ARPES study of the electronic mass enhancement in  $\text{CsV}_3\text{Sb}_5$ [13]. Our estimate for the  $\lambda_{eff}$  in the  $B_{2g}$  pairing state will be lower by 15% or so due to a slightly larger denominator in Eq.(1). For the  $A_{1g}$  pairing state, our estimated  $\lambda_{\max}$  due to charge fluctuations should be supplemented with  $\lambda_{e-p} \approx 0.25$  but the value of  $\mu^* \approx 0.12$  should be taken into account in Eq.(1). This will increase our estimate for  $\lambda_{eff}$  by 10% or so.

To obtain the estimates for the range of charge fluctuational energies that set the scale  $\omega_{cut}$  in the BCS  $T_c$  expression, we calculate Eliashberg spectral functions  $\alpha^2 F(\omega)$  that are responsible for the pairing. Since in our method the Cooper pairs scatter on the statically screened Coulomb interaction,  $\text{Re}K_{\mathbf{k}j, \mathbf{k}'j'}(0)$ , the Kramers-Kronig transformation provides its frequency resolution, proportional to  $\text{Im}K_{\mathbf{k}j, \mathbf{k}'j'}(\omega)/\omega$ . The frequency resolved function  $\text{Im}K_{\mathbf{k}j, \mathbf{k}'j'}(\omega)$  is averaged over the eigenvectors of the BCS gap equation  $\Delta(\mathbf{k}j), \Delta(\mathbf{k}'j')$  to give rise to the superconducting  $\alpha^2 F(\omega)$ , whose double inverse frequency moment evaluates the eigenvalue  $\lambda_{\max}$ . We perform this procedure for the leading eigenstates of  $B_{2g}$  and  $A_{1g}$  symmetries, and also calculate the spectral function  $\alpha_{cf}^2 F(\omega)$  whose inverse moment produces the mass enhancement parameter  $\lambda_{cf}$ .

We present this data in Fig.4, where the black/blue lines show the superconducting  $\alpha^2 F(\omega)$  of the  $B_{2g}$  and  $A_{1g}$  symmetries, respectively, while the red line describes

the charge fluctuational  $\alpha_{cf}^2 F(\omega)$ . A strong peak at the frequencies around 7 meV is seen in all three plots and indicates a characteristic frequency of the charge fluctuations. This can be compared to the Debye frequency of 142K=12 meV deduced from the calculated phonon spectrum of CsV<sub>3</sub>Sb<sub>5</sub>[12].

We can judge about the values of  $T_c$  obtained within the charge fluctuational mechanism using our estimated  $\omega_{cut} \approx 7$  meV and the values of  $\lambda_{eff}$  that we calculate in Fig. 3. For  $\lambda_{eff} = 0.2$ , the BCS  $T_c \approx \omega_{cut} \exp(-1/\lambda_{eff}) \approx 0.5$ K. Once we get closer to the CDW instability, the effective coupling increases to the values 0.4 and the corresponding BCS  $T_c \approx 7$ K. Should the contribution from the phonons be included in the  $A_{1g}$  pairing channel, a refined estimate for  $\lambda_{eff}$  is inflated by about 10% and the BCS  $T_c$ 's are about 20% larger than the values quoted above. Given the exponential sensitivity, these estimates are clearly within the range of the  $T_c$ 's observed experimentally.

In conclusion, we numerically estimated the charge fluctuation mediated pairing tendencies in the recently discovered Kagome metal CsV<sub>3</sub>Sb<sub>5</sub>. These calculations are done directly using first-principle electronic structures without resorting to tight-binding approximations of any kind. Two competing pairing channels have been recovered in our study: the two-fold degenerate  $B_{2g}$  nodal states ( $d_{x^2-y^2}, d_{xy}$  -like) and the non-degenerate  $A_{1g}$  nodeless state (anisotropic s-wave-like) with the effective coupling constants in the range 0.2–0.4 depending on the strength of the nearest neighbor Coulomb repulsion between the vanadium  $d$ -electrons. Similar values are predicted to contribute to the electronic mass enhancement due to charge fluctuations. These estimates provide substantial contributions both to the electronic kinks of the Fermi electrons in the normal state, and to the strength of the Cooper pairing in the superconducting state.

- 
- [1] For a review, see, e.g, C. C. Tsuei and J. R. Kirtley, "Pairing symmetry in cuprate superconductors", *Rev. Mod. Phys.* **72**, 969 (2000).
- [2] For a review, see, e.g, J. Paglione & R. L. Greene, "High-temperature superconductivity in iron-based materials", *Nature Physics* **6**, 645 (2010).
- [3] H. Sun, M. Huo, X. Hu, J. Li, Z. Liu, Y. Han, L. Tang, Z. Mao, P. Yang, B. Wang, J. Cheng, D.-X. Yao, G.-M. Zhang, M. Wang, "Signatures of superconductivity near 80 K in a nickelate under high pressure", *Nature* **621**,493-498 (2023).
- [4] For a review, see, e.g, P. A. Lee, N. Nagaosa, and X.-G. Wen, "Doping a Mott insulator: Physics of high-temperature superconductivity", *Rev. Mod. Phys.* **78**, 17 (2006).
- [5] For a review, see, e.g, D. J. Scalapino, "A common thread: The pairing interaction for unconventional superconductors", *Rev. Mod. Phys.* **84**, 1383 (2012).
- [6] R. J. Cava, B. Batlogg, J. J. Krajewski, R. Farrow, L. W. Rupp, Jr., A. E. White, K. Short, W. F. Peck, and T. Kometani, "Superconductivity near 30 K without copper: the Ba<sub>0.6</sub>K<sub>0.4</sub>BiO<sub>3</sub> perovskite", *Nature* **332**, 814 (1988).
- [7] B. R. Ortiz, L. C. Gomes, J. R. Morey, M. Winiarski, M. Bordelon, J. S. Mangum, I. W. H. Oswald, J. A. Rodriguez-Rivera, J. R. Neilson, S. D. Wilson, E. Ertekin, T. M. McQueen, and E. S. Toberer, New kagome prototype materials: discovery of KV<sub>3</sub>Sb<sub>5</sub>, RbV<sub>3</sub>Sb<sub>5</sub>, and CsV<sub>3</sub>Sb<sub>5</sub>, *Phys. Rev. Materials* **3**, 094407 (2019).
- [8] H. Zhao, H. Li, B. R. Ortiz, S. M. L. Teicher, T. Park, M. Ye, Z. Wang, L. Balents, S. D. Wilson & I. Zeljkovic, Cascade of correlated electron states in the kagome superconductor CsV<sub>3</sub>Sb<sub>5</sub>, *Nature* **599**, 216 (2021).
- [9] B. R. Ortiz, S. M. L. Teicher, Y. Hu, J. L. Zuo, P. M. Sarte, E. C. Schueller, A. M. Milinda Abeykoon, M. J. Krogstad, S. Rosenkranz, R. Osborn, R. Seshadri, L. Balents, J. He, and S. D. Wilson, "CsV<sub>3</sub>Sb<sub>5</sub>: A Z<sub>2</sub> Topological Kagome Metal with a Superconducting Ground State", *Phys. Rev. Lett.* **125**, 247002 (2020).
- [10] B. R. Ortiz, P. M. Sarte, e. M. Kenney, M. J. Graf, S. M. L. Teicher, R. Seshadri, and S. D. Wilson, "Superconductivity in the Z<sub>2</sub> kagome metal KV<sub>3</sub>Sb<sub>5</sub>", *Phys. Rev. Materials* **5**, 034801 (2021).
- [11] K. Y. Chen, N. N. Wang, Q.W. Yin, Y. H. Gu, K. Jiang, Z. J. Tu, C. S. Gong, Y. Uwatoko, J. P. Sun, H. C. Lei, J. P. Hu, and J.-G. Cheng "Double Superconducting Dome and Triple Enhancement of T<sub>c</sub> in the Kagome Superconductor CsV<sub>3</sub>Sb<sub>5</sub> under High Pressure", *Phys. Rev. Lett.* **126**, 247001 (2021).
- [12] H. Tan, Y. Liu, Z. Wang, B. Yan, "Charge Density Waves and Electronic Properties of Superconducting Kagome Metals", *Phys. Rev. Lett.* **127**, 046401 (2021).
- [13] Y. Zhong, S. Li, H. Liu, Y. Dong, K. Aido, Y. Arai, H. Li, W. Zhang, Y. Shi, Z. Wang, S. Shin, H. N. Lee, H. Miao, T. Kondo & K Okazaki, "Testing electron-phonon coupling for the superconductivity in kagome metal CsV<sub>3</sub>Sb<sub>5</sub>", *Nature Communications* **14**, 1945 (2023).
- [14] Z. Liang, X. Hou, F. Zhang, W. Ma, P. Wu, Z. Zhang, F. Yu, J.-J. Ying, K. Jiang, L. Shan, Z. Wang, and X.-H. Chen "Three dimensional charge density wave and surface-dependent vortex-core states in a kagome superconductor CsV<sub>3</sub>Sb<sub>5</sub>", *Phys. Rev. X* **11**, 031026 (2021).
- [15] H.-S. Xu, Y.-J. Yan, R. Yin, W. Xia, S. Fang, Z. Chen, Y. Li, W. Yang, Y. Guo, and D.-L. Feng, Multiband Superconductivity with Sign-Preserving Order Parameter in Kagome Superconductor CsV<sub>3</sub>Sb<sub>5</sub>, *Phys. Rev. Lett.* **127**, 187004 (2021).
- [16] H. Chen, H. Yang, B. Hu, Z. Zhao, J. Yuan, Y. Xing, G. Qian, Z. Huang, G. Li, Y. Ye, S. Ma, S. Ni, H. Zhang, Q. Yin, C. Gong, Z. Tu, H. Lei, H. Tan, S. Zhou, C. Shen, X. Dong, B. Yan, Z. Wang & H.-J. Gao, Roton pair density wave in a strong-coupling kagome superconductor, *Nature* **599**, 222 (2021).
- [17] R. Gupta, D. Das, C. H. Mielke III, Z. Guguchia, T. Shiroka, C. Baines, M. Bartkowiak, H. Luetkens, R. Khasanov, Q. Yin, Z. Tu, C. Gong & H. Lei, "Microscopic evidence for anisotropic multigap superconductivity"

- ity in the CsV<sub>3</sub>Sb<sub>5</sub> kagome superconductor”, npj Quant. Mater. **7**, 49 (2022).
- [18] Z. Shan, P. K. Biswas, S. K. Ghosh, T. Tula, A. D. Hillier, D. Adroja, S. Cottrell, G.-H. Cao, Y. Liu, X. Xu, Y. Song, H. Yuan, and M. Smidman, Muon spin relaxation study of the layered kagome superconductor CsV<sub>3</sub>Sb<sub>5</sub>. Phys. Rev. Research **4**, 033145 (2022).
- [19] M. Roppongi, K. Ishihara, Y. Tanaka, K. Ogawa, K. Okada, S. Liu, K. Mukasa, Y. Mizukami, Y. Uwatoko, R. Grasset, M. Konczykowski, B. R. Ortiz, S. D. Wilson, K. Hashimoto & T. Shibauchi, Bulk evidence of anisotropic s-wave pairing with no sign change in the kagome superconductor CsV<sub>3</sub>Sb<sub>5</sub>, Nature Communications **14**, 667 (2023).
- [20] W. Zhang, X.u Liu, L. Wang, C. W. Tsang, Z. Wang, S. T. Lam, W. Wang, J. Xie, X. Zhou, Y. Zhao, S. Wang, J. Tallon, K. T. Lai, and S. K. Goh, ”Nodeless Superconductivity in Kagome Metal CsV<sub>3</sub>Sb<sub>5</sub> with and without Time Reversal Symmetry Breaking”, Nano Letters **23**, 872 (2023).
- [21] S.-L. Yu and J.-X. Li, Chiral superconducting phase and chiral spin-density-wave phase in a Hubbard model on the kagome lattice, Phys. Rev. B **85**, 144402 (2012).
- [22] W.-S. Wang, Z.-Z. Li, Y.-Y. Xiang, and Q.-H. Wang, Competing electronic orders on kagome lattices at van Hove filling, Phys. Rev. B **87**, 115135 (2013).
- [23] M. L. Kiesel, C. Platt, and R. Thomale, Unconventional Fermi Surface Instabilities in the Kagome Hubbard Model, Phys. Rev. Lett. **110**, 126405 (2013).
- [24] T. Park, M. Ye, and L. Balents, ”Electronic instabilities of kagome metals: Saddle points and Landau theory”, Phys. Rev. B **104**, 035142 (2021).
- [25] X. Feng, Y. Zhang, K. Jiang, and J. Hu, ”Low-energy effective theory and symmetry classification of flux phases on the kagome lattice”, Phys. Rev. B **104**, 165136 (2021).
- [26] Y.-X. Jiang, J.-X. Yin, M. M. Denner, N. Shumiya, B. R. Ortiz, G. Xu, Z. Guguchia, J. He, M. S. Hossain, X. Liu, J. Ruff, L. Kautzsch, S. S. Zhang, G. Chang, I. Belopolski, Q. Zhang, T. A. Cochran, D. Multer, M. Litskevich, Z.-J. Cheng, X. P. Yang, Z. Wang, R. Thomale, T. Neupert, S. D. Wilson, and M. Z. Hasan, ”Unconventional chiral charge order in kagome superconductor KV<sub>3</sub>Sb<sub>5</sub>”, Nature Materials **20**, 1353 (2021)
- [27] S. Y. Savrasov, G. Resta, X. Wan, ”Local self-energies for V and Pd emergent from a nonlocal LDA+FLEX implementation”, Phys. Rev. B **97**, 155128 (2018).
- [28] G. Heier, S. Y. Savrasov, ”Calculated Spin Fluctuational Pairing Interaction in HgBa<sub>2</sub>CuO<sub>4</sub> using LDA+FLEX Method”, Phys. Rev. B **109**, 094506 (2024).
- [29] For a review, see, e.g., Theory of the Inhomogeneous Electron Gas, edited by S. Lundqvist and S. H. March (Plenum, New York, 1983)..
- [30] For a review, see, e.g, G. Kotliar, S. Y. Savrasov, K. Haule, V. S. Oudovenko, O. Parcollet, C.A. Marianetti, ”Electronic structure calculations with dynamical mean-field theory”, Rev. Mod. Phys. **78**, 865, (2006).
- [31] N. E. Bickers, D. J. Scalapino and S. R. White, ”Conserving Approximations for Strongly Correlated Electron Systems: Bethe-Salpeter Equation and Dynamics for the Two-Dimensional Hubbard Model”, Phys. Rev. Lett. **62**, 961 (1989).
- [32] G. Heier, K. Park, S. Y. Savrasov, Competing  $d_{xy}$  and  $s_{\pm}$  Pairing Symmetries in Superconducting La<sub>3</sub>Ni<sub>2</sub>O<sub>7</sub>: LDA+FLEX Calculation, Phys. Rev. B **109**, 104508 (2024)
- [33] S. Y. Savrasov, ”Linear-response theory and lattice dynamics: A muffin-tin-orbital approach”, Phys. Rev. B **54**, 16470 (1996).
- [34] A. S. Alexandrov, ”Unconventional pairing symmetry of layered superconductors caused by acoustic phonons”, Phys. Rev. B **77**, 094502, (2008)